

The Data-Directed Paradigm for BSM searches

Sergey Volkovich^{1,a}, Federico De Vito Halevy¹, Shikma Bressler¹

¹Department of Particle Physics & Astrophysics, Weizmann Institute of Science, Rehovot, Israel

Received: date / Accepted: date

Abstract In search for new physics, we must leave no stone unturned. We propose a novel data-directed paradigm (DDP) for developing Beyond the Standard Model (BSM) signal hypotheses on the basis of collected data. The DDP is complimentary to traditional theory-directed searches that follow the blind-analysis paradigm and could open the door to regions in the data that will otherwise remain vastly unexplored. We suggest looking directly at the data to identify exclusive selections which exhibit significant deviations from some unique feature of the Standard Model. Such regions should be considered well-motivated for data-directed BSM hypotheses and studied further. In this letter, the paradigm is demonstrated by combining the promising potential of machine learning algorithms with the commonly used search for excesses of events over a smoothly falling background (bump-hunting). A deep neural network is trained to map any invariant mass distribution into a z -distribution that indicates the presence of statistically significant bumps. Using this approach, the time and effort consuming tasks of background and systematic uncertainty estimation are avoided. Compared to identifying bumps with the profile-likelihood ratio test using perfectly known background and signal, the algorithm is inferior by only 5%.

Introduction. Despite its great success in describing the elementary particles and their interactions, the Standard Model (SM) is still incomplete [1]. Many models extending beyond the Standard Model (BSM) have been developed over the years predicting the existence of new resonances. Thus, the search for new resonances, either theoretically-predicted or model-agnostic, is a

core strategy for discovery in experimental high energy physics (e.g. recently [2,3,4]).

With no exception, all such searches have been conducted following the blind-analysis paradigm, in which an enormous amount of time and effort is invested, i.e. on background modeling and systematic uncertainty estimation, before looking at the data. However, the resource-intensive tasks required to perform these searches have allowed only a limited region in the space spanned by all observables (“observable-space”) to be covered to-date. Indeed, searches typically focus on inclusive final states — di-lepton, di-photon, di-jet, etc. — ignoring all other observables and avoiding exclusive selections such as di-lepton + jets, di-jets + missing transverse momentum, di-photon within a $t\bar{t}$ topology, etc.. Moreover, within the studied final states, event selection was optimized relative to predefined signal models. So far, no indication of BSM physics has been found.

Complimentary to the blind analysis paradigm, we propose a data-directed paradigm (DDP). The strategy consists of quickly searching the observable-space for exclusive regions exhibiting a significant deviation from some fundamental SM property. Such regions should be considered for data-directed signal hypotheses and further examined using traditional analysis techniques. Given the large number of plausible signals which could manifest in an infinite number of exclusive regions, and moreover, the limited time, manpower and resources at hand, the proposed DDP might provide our best chance at discovering BSM physics.

The Data-Directed Paradigm. A search in the DDP can be implemented with two key ingredients:

1. A property unique to the SM with respect to which deviations can be searched for — here we exploit the fact that within the SM, in absence of resonances,

^aCorresponding author: volkovich.sergey@weizmann.ac.il

almost any invariant mass distribution is smoothly falling.

2. An efficient algorithm to scan the observable-space in search for deviations — here we train a deep neural network (NN) to map any invariant mass distribution into a distribution of statistical significance for excesses of events (“bumps”). The latter is known as a “ z ” distribution and is based on the profile likelihood ratio test for positive signals [5].

As long as the underlying background distribution is smoothly falling, a single trained NN, as described in this letter, is able to perform statistical inference from any selection of observed data. Thus avoiding the time- and effort-consuming tasks of full background and systematic uncertainty estimation. This way, a potentially unlimited quantity of exclusive invariant mass distributions can be scanned and large regions in the observable-space can be covered. Nevertheless, we note that event-by-event optimization for bump enhancement, as studied for instance in [6, 7, 8, 9], is left to future work.

Bumps identified using the DDP are likely to be caused by statistical fluctuations. These will be washed out when tested with more data. Bumps originating from systematic uncertainties due to detector effects (trigger thresholds, kinematic edges, etc.) are expected to appear in Monte Carlo simulations as well and can be ruled out. Systematic uncertainties not modeled by the simulation are expected to be experiment-specific, and could be looked for by other experiments. Identified bumps which do not disappear with additional data, do not appear in the simulation and appear in more than one experiment, should be considered as BSM signal hypotheses and devoted a dedicated analysis.

A neural net implementation. The NN is trained in a supervised manner, for which we generate a set of artificial training and testing data. These comprise inputs which simulate realistic and complete distributions in observed data (in contrast to individual events, as in [6, 7, 8, 9]), matched to analytically calculated z distributions as targets. When given an invariant mass distribution, the NN predicts a z distribution which shows where and how likely it is that the data contains a bump. Once the NN has been trained, we validate that its predictions are consistent and that its loss value converges. Finally, its predictions are evaluated on the test set and we discuss its performance.

We generate the inputs of the NN such that they represent a 100 bin histogram of observed events, $N = B + S$. The generation process is illustrated in Fig. 1. Each input is composed of a smoothly decaying background curve, B , to which Poisson fluctuations are added, and a localized Gaussian signal, S , whose significance is defined relative to the fluctuated background. We then

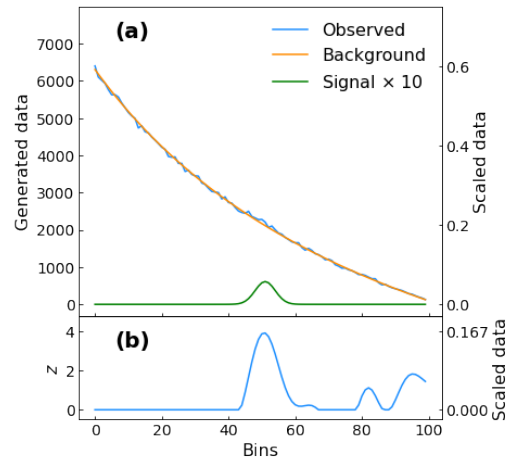


Fig. 1 Illustration of the sample generation procedure. (a) A smoothly decaying background curve (*orange*) is generated over 100 bins. Each bin is assigned a Poisson fluctuation. A signal with a significance relative to the fluctuated background (*green*) is added to it, producing the observed data (*blue*). (b) The corresponding significance distribution, z , is calculated analytically. The left and right axes in both panels show the non-scaled and scaled distributions, respectively.

calculate bin-by-bin the corresponding NN target, z , which we use to approximate the significance distribution given the unfluctuated background and assuming a Gaussian signal shape [5]. Each input and target pair is collectively referred to as a “sample”. All samples are then globally scaled to the interval $[0, 1]$ under a linear transformation and used to train the NN.

A variety of smoothly falling backgrounds is modelled by randomly selecting one of the following ten functional forms for each sample:

$$\begin{aligned}
 & be^{-ax}, \quad ax + b, \quad \frac{1}{ax} + b, \quad \frac{1}{ax^2} + b, \quad \frac{1}{ax^3} + b, \\
 & \frac{1}{ax^4} + b, \quad a(x - x_2)^2 + y_2, \quad -a \cdot \ln(x) + b, \\
 & (y_1 - y_2) \cos(a(x - b)) + y_2, \quad \cosh(a(x - x_2)) + b.
 \end{aligned} \tag{1}$$

The parameters a and b are defined such that each curve decays between two points, (x_1, y_1) and (x_2, y_2) , where $x_1 < x_2$ are the centers of the extreme bins and $y_1 > y_2$ are randomized from the interval $[100, 10000]$.

To avoid edge effects, Gaussian shaped signals are generated with mean values distributed randomly between bin 25 and bin 75. The width of the signals is fixed at 3 bins. To improve the desired feature detection, the NN is trained with a data set containing signals with significance in the range $[1, 20]\sigma$. The performance of the NN is determined by evaluating its ability to identify bumps with a significance of 3σ — the common definition of a “hint” for BSM physics.

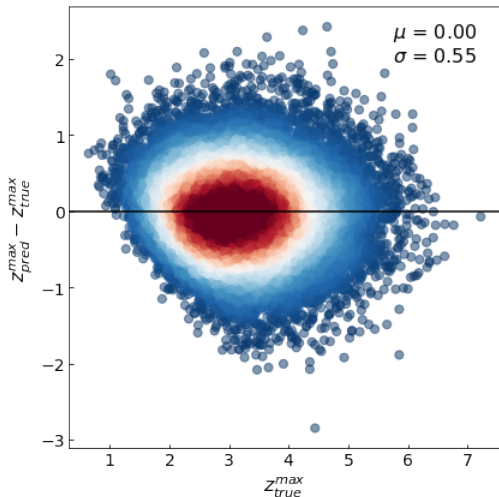


Fig. 2 The difference between z_{pred}^{max} and z_{true}^{max} as a function of z_{true}^{max} . Dense regions are shown in red (roughly corresponding to the 1σ region), while sparse regions are shown in blue.

Various NN architectures can be used and the search for an optimal one is left to a later stage. Here, we choose an architecture based on a dense layer followed by six 1-dimensional convolutional layers. The latter are intended for feature-detection, while the former is useful in suppressing position-dependent biases. Our resulting network possesses a total of 73,941 trainable parameters. A “rectified linear unit” activation function is used on all layers. The “Adam” optimizer is used to minimize the “mean squared error” loss function. Minimization is iterated over 200 epochs at a learning rate of 0.0003 and a batch size of 100. We generate a total of 600,000 training samples, 20% of which are used for validation, and 25,000 testing samples.

Results. The accuracy of the NN prediction is illustrated in Fig. 2 in terms of the difference between the maximal predicted significance, z_{pred}^{max} , and the one calculated via the profile likelihood ratio test, z_{true}^{max} , versus the latter. All generated test samples are included in the figure; in over 90% of these the predicted peak was found within 3 bins of z_{true}^{max} . A mean (μ) of 0 indicates a negligible bias in the prediction and a 0.55 standard deviation (σ) measures its precision. The asymmetry seen as a sharp edge in the third quadrant originates from the small number of maximal z predictions below one.

We are interested in finding samples with bumps of 3σ significance while rejecting samples without bumps. Fig. 3 shows z_{true}^{max} in solid line and z_{pred}^{max} in dashed line for samples with no signal added (blue) and for samples with a 3σ significance signal added (orange). In a traditional bump-hunting search, the signal significance is evaluated relative to an estimated background. Thus,

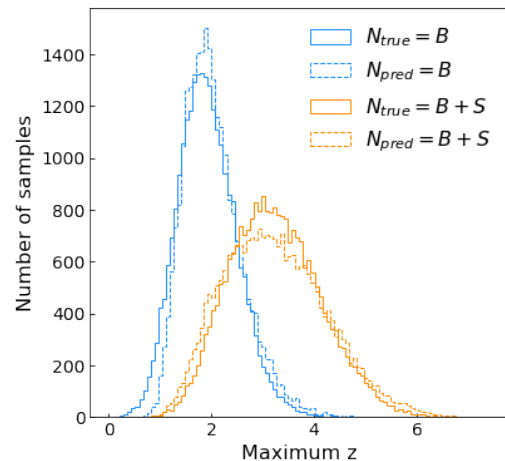


Fig. 3 The distribution of z_{true}^{max} (solid line) and z_{pred}^{max} (dashed line) for samples with no signal added (blue) and for samples with a 3σ significance signal added (orange)

the measured significance of a 3σ signal could fluctuate around this value. This is the origin of the width of the z_{true}^{max} distributions: the signal is generated with significance relative to the fluctuated background and its z_{true}^{max} is evaluated relative to the smooth background.

According to the Neyman-Pearson lemma (see e.g. [10]), z_{true}^{max} provides the most powerful signal to background separation. It relies on exact knowledge of both the background and signal shapes. Yet, despite using no a priori knowledge of the two, the signal to background separation in z_{pred}^{max} is only slightly degraded relative to z_{true}^{max} . This is quantified in terms of receiver operating characteristic (ROC) curves in Fig. 4, obtained from the distributions of Fig. 3. The true (blue) and predicted (orange) ROC curves show the efficiency to correctly identify a 3σ bump versus the false positive rate of selecting samples with no bumps. The area under the true curve, A_{true} , is 0.897 while the area under the predicted curve, A_{pred} , is 0.855, which implies a degradation in performance of less than 5%.

We also confirmed that the NN is able to generalize to identifying with similar accuracy bumps over linear combinations of the background forms (Eq. 1). Similar performance was obtained when training and testing on samples with wider bumps, of either 4 or 5 bins.

Validation. We validate the convergence of the loss value achieved by increasing either the number of epochs or the size of the training data set. In terms of A_{pred} from Fig. 4, the NN performance varies insignificantly, by less than 1% when moving past 200 epochs (100,000 input samples) or 500,000 input samples (100 epochs).

Consistency was ensured by comparing the NN predictions in two scenarios (with 100,000 training samples and 100 epochs). First, we trained four different

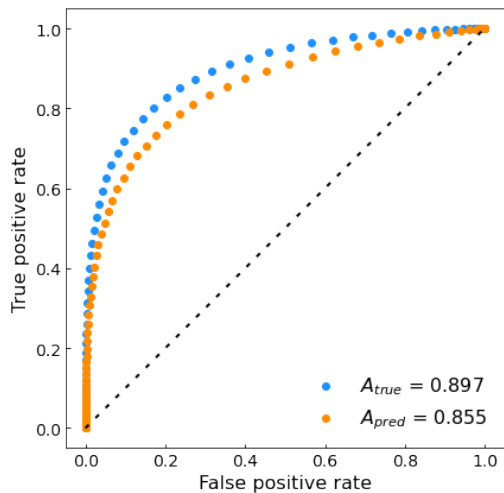


Fig. 4 True (blue) and predicted (orange) ROC curves and their associated areas under curve, A_{true} and A_{pred} .

NNs using an independent training data set for each and compared their predictions on a common testing data set. Despite small variations in the average bias ($\mu \in [0.06, 0.34]$), their predictive precision remained excellent ($\sigma \in [0.74, 0.8]$). Therefore, our overall ability to separate signal from background was unaffected ($A_{\text{pred}} \in [0.82, 0.83]$). Second, the performance of each of the NNs was separately compared on four different testing data sets. In all cases, the precision and bias varied negligibly. Consequently, the accuracy when separating signal from background was again unaffected.

Discussion. We have presented a novel data-directed paradigm, complementary to the blind analysis paradigm, and demonstrated one of its possible implementations using the concept of bump-hunting. We have shown that a NN can be trained to efficiently identify bumps over smoothly falling backgrounds without being given any a priori information about the background or the bump’s position. Relative to the most powerful test statistic (profile likelihood ratio), which relies on exact knowledge of both the background and signal shapes, the performance of the NN was only inferior by less than 5%. These results pave the way towards scanning the overwhelming observable-space that is being measured in experiments searching for bumps. Examples could be searches for di-lepton, di-jet, di-photon, jet-lepton-missing E_T resonances in events containing, in addition, any other set of objects.

Testing the performance of other, more sophisticated NN architectures, as well as generalizing this work to other smooth background forms are left for future work. One conceptual limitation of the current procedure is that the NN target is not an inherent property of the observed data alone, but also of the smooth

background and signal shapes. A procedure where the smooth background is estimated first and then used as an input as well is certainly worth exploring.

In the search for BSM physics we must leave no stone unturned. Complementary to traditional theory-directed blind analysis searches, the DDP should be pursued as well. With the expected ramp up of the Large Hadron Collider, existing data should be thoroughly explored. A first milestone could be demonstrating sensitivity to bumps in regions already investigated. The search for bumps over smoothly falling backgrounds is just one example of a property of the SM that could be considered. Other properties such as flavour symmetry [11] or forward-backward symmetry could be exploited as well. Given the challenge ahead, the proposed DDP might provide our best chance at discovering BSM physics.

Declarations Funding This work was supported by Grant No. 2871/19 from the Israeli Science Foundation (ISF), Grant No. I-1506-303.7/2019 from the German Israeli Foundation (GIF) and by the Sir Charles Clore Prize. **Conflicts of interest / Competing interests** The authors have no conflicts of interest to declare that are relevant to the content of this article.

Availability of data and material The datasets generated and analysed during this work are available from the corresponding author on reasonable request.

Code availability The code of this work is available from the corresponding author on reasonable request.

References

1. S. Weinberg, Phys. Rev. Lett. **121**, 220001 (2018)
2. ATLAS Collaboration, JHEP **03**, 145 (2020)
3. ATLAS Collaboration, Phys. Lett. B **796**, 68-87 (2019)
4. ATLAS Collaboration, Phys. Rev. Lett. **125**, 051801 (2020)
5. G. Cowan, K. Cranmer, E. Gross, O. Vitells, Eur. Phys. J. C **71**, 1554 (2011)
6. ATLAS Collaboration, Eur. Phys. J. C **79**, 120 (2019)
7. J. Collins, K. Howe, B. Nachman, Phys. Rev. Lett. **121**, 241803 (2018)
8. M. Farina, Y. Nakai, D. Shih, Phys. Rev. D **101**, 075021 (2020)
9. J. Collins, K. Howe, B. Nachman, Phys. Rev. D **99**, 014038 (2019)
10. E.L. Lehmann, J.P. Romano, *Testing Statistical Hypotheses*, 3rd edn. (Springer, New York, 2005)
11. S. Bressler, A. Dery, A. Efrati, Phys. Rev. D **90**, 015025 (2014)